Mutual Diffusion in Blends of Long and Short Entangled Polymer Chains

Elizabeth A. Jordan,[†] Robin C. Ball,[†] Athene M. Donald,[†] Lewis J. Fetters,[‡] Richard A. L. Jones,[†] and Jacob Klein*[§]

Cavendish Laboratory, Cambridge CB3 OHE, England, Corporate Research—Science Laboratories, Exxon Research and Engineering Corporation, Clinton Township, Annandale, New Jersey 08801, and Polymer Department, Weizmann Institute of Science, Rehovot 76100, Israel. *Received March 30, 1987*

ABSTRACT: We have used infrared microdensitometry to study the mutual diffusion across an originally sharp interface between two saturated polybutadienes of degrees of polymerization N_A and N_B ($\gg N_e$, the entanglement length) for three different ratios N_A/N_B. The extent of diffusion broadening suggests that the mutual diffusion coefficient is controlled by the mobility of the *faster moving* (shorter) polymer chains, indicating that convective flow may be important in such mixing phenomena.

I. Introduction

Self-diffusion and tracer diffusion in polymer melts has been extensively studied in recent years.[1] For highly entangled linear polymers of degree of polymerization N_A the self-diffusion coefficient D_A is well described by the reptation relation[2,3]

$$D_A = (N_e B_0 k_B T)/N_A^2 \quad (1)$$

where N_e is the entanglement degree of polymerization for the polymer ($N_A \gg N_e$), B_0 a monomer mobility, and k_B and T are Boltzmann's constant and temperature.

There is considerably less consensus on diffusion in blends of different polymers, to some extent because few direct experimental studies in such systems have been available. Recent investigations of the mutual diffusion coefficient in compatible polymer mixtures include studies by Gilmore et al.[4] and by Jones et al.[5] on the binary blend poly(vinyl chloride)/polycaprolactone using electron microscopy methods, by Composto et al.[6] on the polystyrene/poly(phenylene oxide) blend and by Sokolov et al.[7] on the solution-chlorinated polyethylene/poly(methyl methacrylate) blend using particle scattering techniques, and by Murschall et al.[8a] and Brereton et al.[8b] on the poly(phenylmethylsiloxane)/polystyrene system using short polymers (20–90 monomers) and a light scattering approach. Earlier studies using an electron microscopy method of interdiffusion in the PVC/PMMA system by Kamenskii et al.[9b] and by Chalykh et al.[9a] should be noted.

For two polymers A and B the Flory–Huggins free energy of mixing is[10]

$$F/k_B T = (\phi_A/N_A) \log \phi_A + (\phi_B/N_B) \log \phi_B + \chi \phi_A \phi_B \quad (2)$$

where ϕ_A and ϕ_B are the respective polymer volume fractions, χ is the segmental interaction parameter, and in the bulk $\phi_A + \phi_B = 1$. For compatible polymers (where the segmental interaction parameter χ may be large and negative) the attractive interactions between A and B monomers, when summed over the polymer chains, lead to a large enthalpic driving force favoring mixing.[11] The resulting mutual diffusion coefficient is then strongly composition dependent and considerably enhanced relative to the intrinsic or self-diffusion coefficients of either A or B.[5,6] In this paper we investigate a related question, that of mutual diffusion in a blend of A and B chains, where the A and B monomers are identical ($\chi = 0$) but the polymers differ in molecular weight, so that

$$N_A > N_B \gg N_e \quad (3)$$

A number of theoretical treatments of this problem (for $\chi = 0$) have appeared in recent years and it will be of value to summarise them briefly here. All are based on an effective driving force for mixing deriving from eq 2 but contain somewhat different assumptions regarding the mechanism of diffusion. Extending an earlier discussion by de Gennes,[11a] Brochard et al.[12] analyzed the diffusion broadening of an N_A/N_B couple. The incompressibility condition assumed in their calculation amounted to a requirement that, in order for a short N_B chain to diffuse, it was necessary for a longer N_A chain to move away (also by diffusion) to create the necessary free volume. This results in a strong coupling of the mutual diffusion coefficient $D_1(\phi)$ to both D_A and D_B:

$$D_1(\phi) = D_0[\phi(1 - R) + R]/[1 - \phi(1 - R)] \quad (4)$$

where $D_0 = (D_A D_B)^{1/2}$, $R = N_B/N_A$ ($R < 1$), and we have written $\phi_A = \phi = 1 - \phi_B$ for clarity.

A different approach was taken by Kramer and coworkers.[13] They used a lattice model, in analogy with treatments of diffusion in crystalline solids, where a vacancy flux allowed bulk flow to take place. The resulting mutual diffusion coefficient $D_2(\phi)$ (for interdiffusion across the interface between the N_A,N_B couple) had the form

$$D_2(\phi) = D_B[\phi + R(1 - \phi)]^2 \quad (5)$$

i.e., the magnitude of the mutual diffusion coefficient is comparable to the self-diffusion coefficient D_B of the *faster* moving (shorter) species over an appreciable composition range. Experiments to measure the displacement $\Delta x(t)$ at time t of "markers" positioned at the interface between two polystyrene samples of lengths N_A (large and fixed) and N_B for three values of R showed

$$\Delta x(t) \propto (D_B t)^{1/2} \quad (6)$$

a variation consistent with the form (5) for the mutual diffusion coefficient.

The vacancy-flux approach for analyzing the broadening of the N_A/N_B interface was subsequently criticized by Brochard and de Gennes,[14] on the grounds that it would lead to unacceptable density gradients in the sample. They suggested that up to a time τ_A, the reptation time of the longer N_A chains, the N_A side of the couple would be swollen by the shorter chains at a rate controlled by D_B. Since the relevant length scales $l \simeq (D_B \tau_A)^{1/2} \simeq 1$–$20$ μm

* To whom all correspondence should be addressed.
† Cavendish Laboratory.
‡ Exxon Research and Engineering Corporation.
§ Weizmann Institute, Incumbent, Herman Mark Chair of Polymer Physics.

0024-9297/88/2221-0235$01.50/0

Table I
Molecular Characteristics of Precursor PBD Polymers[a]

sample	$M_w \times 10^{-4}$	M_w/M_n	$(N/N_e)^b$
LF-14	3.2	1.03	27
LF-15	10.6	1.06	88
JK/LF-1	20.0	1.05	167
DSP-1	54.0	1.06	450

[a] The molecular weights were determined by light scattering (M_w) and size-exclusion chromatography (M_n). [b] The number of entanglement lengths per molecules is for the corresponding *saturated* PBD, taking[29] $N_e = M_w/1.2 \times 10^3$.

were in all cases greater than the Δx values measured, this transient swelling would account for the marker-displacement results. This suggestion implies that any experiment whose spatial range is less than or comparable with l will also fall within the transient swelling regime (where the swelling is always controlled by the more rapid D_B).

More recently the vacancy flux mechanism was analysed by Binder;[15] he showed that if an equilibrium vacancy concentration was introduced in a self-consistent way, not only into the flux equations but also into the *mixing free energy* (eq 2), then the mutual diffusion coefficient reverts to the form $D_1(\phi)$ (eq 4) proposed by Brochard et al. rather than the form $D_2(\phi)$ (eq 5).

Yet a third approach was taken by Sillescu,[16] who applied the classical theory for interdiffusion in binary liquid mixtures, with certain simplifying assumptions, to evaluate the mutual diffusion coefficient in the N_A,N_B system considered above. His treatment again used the Flory–Huggins expression, eq 2, for the mixing free energy, but without the need to invoke vacancy flux. Sillescu finds that the mutual diffusion coefficient in this case becomes identical with $D_2(\phi)$, eq 5.[16b] The essential difference between the Sillescu and Brochard et al. analyses is the inclusion of a convective term in the former which maintains the incompressibility conditions; the physical picture is then one where the shorter chains diffuse into the region of longer chains, and these latter move by convection in the opposite direction to maintain constant density. More recent treatments by Ball[17] and Jones,[18] where convective flows are explicitly introduced into the flux equations, recover the Sillescu result at long times.

In the present study we use an experimental approach to investigate the mutual diffusion across the interface between two polymers with chemically identical microstructures but of different degrees of polymerization N_A and N_B. Such a system is of interest not only in the context of the foregoing discussion but also as a model for the more general problem of how two polymers interdiffuse when their mobilities differ widely. In several of the earlier investigations[4-6,8] pairs of polymers with widely differing glass transition temperatures were used, which necessitated assumptions in the theoretical interpretation of the data. This problem clearly does not arise in the present case. In section II we describe the experiments, and in section III we critically compare our experimental diffusion-broadened profiles with these calculated on the basis of the predicted mutual diffusion coefficients arising from the various theoretical approaches.

II. Materials and Methods

The polymers used in this study are polybutadienes (PBD), saturated by catalytic high-pressure hydrogenation or deuteriation of the anionically polymerized PBD precursor chains (92% 1,4-isomer, 8% 1,2-isomer), leading to PBD-*h* and PBD-*d*, respectively.[19,20] Their characteristics are given in Table I. Infrared analysis was used to confirm complete saturation of each sample (i.e., the absence of a peak due to the double bond at 965 cm^{-1}).

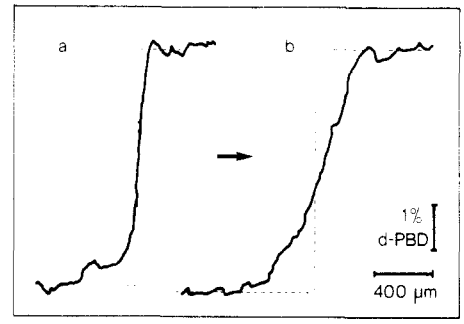

Figure 1. Typical concentration–distance profile $\phi(x)$ (a) immediately following creation of step-function between a film of hydrogenated PBD, $M = 5.4 \times 10^5$, and a film of 95% hydrogenated PBD/5% deuteriated PBD, both of $M_w = 3.2 \times 10^4$ (b) $\phi(x)$ following diffusion broadening at 176 ± 0.5 °C. for 1.21×10^6 s. The thin broken lines in both a and b represent the "ideal" step-function. The half- or interquartile-width of the experimental step function (a) (i.e., the width between $\phi(x) = \phi_0/4$ and $3\phi_0/4$, where $\phi_0 = 5\%$ is the height of the step) is ~55 μm, while the half-width of the broadened profile (b) is ~310 μm.

The resulting saturated polymers have a polyethylene-like structure, with ca. 18 ethylene side groups per thousand main-chain carbon atoms.[19]

We use infrared microdensitometry[21] (IRM) to observe the broadening with time of an originally sharp interface between two polymers in a couple as they interdiffuse. The shape and width of the resulting diffusion-broadened profile is recorded directly and contains information on the magnitude and concentration dependence of the mutual diffusion coefficient.[22]

The thin-film IRM technique was used:[23] squares of the two polymers (5 mm × 5 mm × 140 μm) were prepared by molding small quantities of each material between poly(tetrafluoroethylene) (PTFE) spacers in a vacuum oven. A sharp interface was then created between the N_A and N_B polymers by placing the squares adjacent to each other in a rectangular PTFE former and sandwiching the couple thus formed between layers of PTFE and glass slides, as described previously. The N_A ($>N_B$) side of the polymer couple consisted of 100% hydrogenated chains, while the N_B side was composed of 5% PBD-*d* and 95% PBD-*h*. The diffusion couple was sealed under an atmosphere of nitrogen and interdiffusion took place at 176 ± 0.5 °C for varying periods (ca. 2 weeks). At the end of each run the extent of broadening was measured by scanning across the sample by using IRM at the absorption frequency of the C–D stretching peak.[21] Typical concentration–distance ($\phi(x)$) profiles are shown in Figure 1. The experimentally measured (interquartile) width of the initial step function (Figure 1a) varied (as in previous studies using IRM[21]) between 40 and 80 μm, due mainly to the finite width of the slit in the IR microdensitometer, while the final diffusion-broadened profiles had interquartile widths at least 5 times this value in all experiments (see also Figure 1b and Figures 2–4). We note that in the determination of the initial step function (Figure 1a) the couple was first melted and then rapidly quenched. Thus any spurious broadening effects resulting from volume changes on melting and solidifying of the sample are included in the initial step function width and are therefore small compared with the final broadened profiles.

III. Results and Discussion

Figures 2–4 show typical profiles obtained after diffusion broadening of the N_A/N_B couples for the three values of R (Table I). For an incompressible binary system with a concentration-dependent mutual diffusion coefficient $D(\phi)$ the interdiffusion equation in one dimension is[22]

$$\partial\phi(x,t)/\partial t = \partial/\partial x(D(\phi)\ \partial\phi/\partial x) \qquad (7)$$

where ϕ is the concentration of one of the components (at x and t) and for a binary couple as in our experiments the boundary conditions on eq 7 are $\phi = 0$ at $x = -\infty$ and $\phi = 1$ at $x = +\infty$ for all t. Equation 7 has been solved for ϕ by Brochard et al.[12] for $D = D_1(\phi)$ (eq 4) and by Kramer

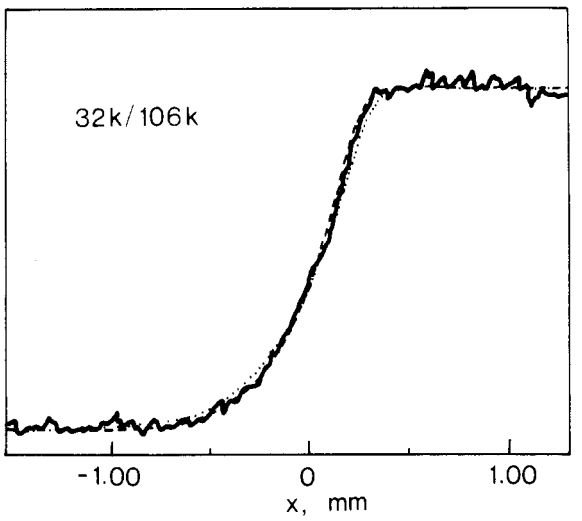

Figure 2. Typical concentration–distance profile ($\phi(x)$) for the couple $3.2 \times 10^4/1.06 \times 10^5$ ($R = 0.30$) following diffusion-broadening for 1.21×10^6 s at 176 ± 0.5 °C. The broken curve and the dotted curve represent profiles calculated on the basis of $D_1(\phi)$ (eq 4) and $D_2(\phi)$ (eq 5), respectively.

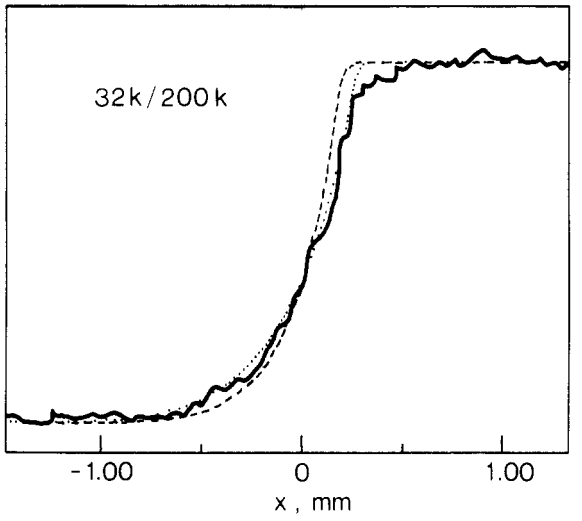

Figure 3. Typical concentration–distance ($\phi(x)$) profiles for the couple $3.2 \times 10^4/2.0 \times 10^5$ ($R = 0.16$) following diffusion broadening for 1.21×10^6 s at 176 ± 0.5 °C. The broken and dotted curves are profiles calculated on the basis of $D_1(\phi)$ and $D_2(\phi)$, respectively.

et al.[13] for $D = D_2(\phi)$ (eq 5), for selected values of R. Theoretical profiles for these two functional forms of $D(\phi)$ for the values of R in our experiments were generated by using a rapidly converging iteration procedure (see Appendix) and checked against profiles calculated for different R values by Brochard et al.[12] and Kramer et al.[13]

In Figures 2–4 are shown computed curves based on the values of R used in the present study ($R = 0.30$, 0.16, and 0.059 for Figures 2, 3, and 4, respectively). The values of D_A and D_B (for self-diffusion of the N_A and N_B saturated PBD chains) used in scaling these theoretical profiles were taken from the tracer diffusion data for linear deuteriated PBD diffusing at 176 °C from ref 20,

$$D_i = D_L N_i^{\alpha} \tag{8}$$

where $D_L = 2.8 \times 10^{-3}$ cm^2 s^{-1}, $\alpha = 1.95$, and i = A or B; N_i here is the number of backbone carbon atoms in the polymer chain. The tracer diffusion coefficient D_B of PBD-*d*, $M_w = 3.2 \times 10^4$, diffusing in PBD-*h* of $M_w = 5.4 \times 10^5$ (at 2% w/w of the shorter molecules at 176 °C), was measured by using IRM, to check the validity of eq 8 for

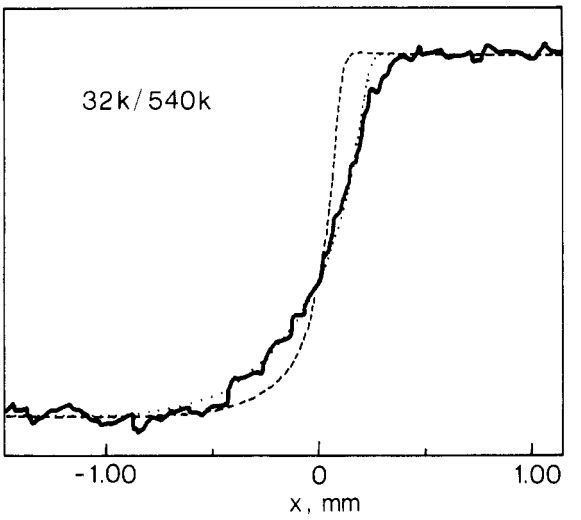

Figure 4. Typical concentration–distance ($\phi(x)$) profile for the couple $3.2 \times 10^4/5.4 \times 10^5$ ($R = 0.059$) following diffusion broadening for 1.21×10^6 s at 176 ± 0.5 °C. Broken and dotted curves are profiles calculated on the basis of $D_1(\phi)$ and $D_2(\phi)$, respectively. The profile is from a different experiment than that shown in Figure 1b; within the scatter, the two experimental curves are closely superimposable.

Table II
Theoretical and Experimental Half-Width $W_{1/2}$, in μm

M_A/M_B	$W_{1/2}$[a] (exptl)	$W_{1/2}$ ($D=D_1(\phi)$)[b]	$W_{1/2}$ ($D=D_2(\phi)$)[b]
$106 \times 10^3/32 \times 10^3$	330 ± 20	309 ± 20 (266)	370 ± 25 (318)
$200 \times 10^3/32 \times 10^3$	330 ± 20	221 ± 15 (190)	329 ± 20 (283)
$540 \times 10^3/32 \times 10^3$	335 ± 30	129 ± 10 (111)	298 ± 20 (256)

[a] Based on between 3–5 experiments for each couple (6–10 experimental profiles). [b] Calculated by using D_A, D_B values from eq 8, where error is based on estimated error in D_L (eq 8). Values in parentheses are calculated by using D_A, D_B values scaled down to take account of possible matrix effects (see text following eq 8).

this study. The value obtained, $D_B = 5.4 \times 10^{-10}$ cm^2 s^{-1}, is lower than that obtained by interpolation from eq 8, $D_B = 7.3 \times 10^{-10}$ cm^2 s^{-1}. The difference is a little larger than the estimated error in D_L[20] and suggests a slight matrix effect (the matrix used in establishing eq 8 was a polydisperse linear polyethylene). D_B compares more closely with the self-diffusion coefficient interpolated for such a molecular weight from the study (on PBD-*d*/PBD-*h* melts) by Bartels et al.[24] (for which $D_B = 5.6 \times 10^{-10}$ cm^2 s^{-1} at 176 °C). The effect on the theoretical profiles of using these differing values of D_B is small (see also Table II).

Examination of the experimental profiles (solid lines in Figures 2–4) reveals a distinct assymmetry in the profiles, with considerably more broadening on one side of the original interface (the N_A side, penetrated by the more rapidly diffusing N_B chains) than on the other: this is due to the large disparity between D_A and D_B (which scales as R^2) and was noted by both Brochard et al. and by Kramer et al. when they presented the calculated concentration profiles deriving from eq 7 for $D_1(\phi)$ and $D_2(\phi)$, respectively (we note that such asymmetry is absent from earlier IRM studies when $N_A = N_B$[21]). Comparison of the experimental concentration–distance profiles of Figures 2–4 for the three R values with those generated from eq 7 shows that the theoretical profiles corresponding to $D_2(\phi)$ (dotted curves) are closer to the experimental IRM profiles than those corresponding to $D_1(\phi)$ (dashed curves). This is less marked for the $3.2 \times 10^4/10.6 \times 10^4$ couple (Figure 2) but is quite noticeable for the 3.2×10^4 couple (Figure 3) and is particularly striking for the $3.2 \times 10^4/5.4 \times 10^5$ couple (Figure 4, $R = 0.059$). This comparison strongly suggests

Table III
Values of $\beta_{R,i} = W_{1/2}(4D_i(1/2)t)^{1/2}$ (i = 1 or 2) where $W_{1/2}$ Is Interquartile Width of the Diffusion Broadened Step-Function Following a Time t with Mutual Diffusion Coefficient $D_i(\phi)$

M_A/M_B	$R = N_B/N_A$	$\beta_{R,1}$	$\beta_{R,2}$
$106 \times 10^3/32 \times 10^3$	0.30	1.12	1.10
$200 \times 10^3/32 \times 10^3$	0.16	1.16	1.11
$540 \times 10^3/32 \times 10^3$	0.059	1.26	1.13

[a] For a ϕ-independent diffusion coefficient (R=1), $\beta_{R,i} = \beta_0 = 1.10$.

that the interpenetration across the N_A/N_B interface is controlled by a mutual diffusion coefficient with a form given by $D_2(\phi)$.

The main difference between the theoretical profiles based on the two forms of $D(\phi)$ is in their *width* rather than their shape: we expect those based on $D_1(\phi)$ to have a width characterized by $(D_0t)^{1/2}$, where t is the time of diffusion broadening and D_0 is the geometric mean of D_A and D_B; while the concentration–distance profiles generated on the basis of $D_2(\phi)$ have a width characterized by $(D_Bt)^{1/2}$. By use of our data to discriminate between the two forms of $D(\phi)$, then, it is the *broadening* of the profiles that must be especially scrutinized, rather than their shape alone. A particularly useful quantitative measure of this broadening is the interquartile width $W_{1/2}$, which is the width between the $\phi = {}^1/_4$ and $\phi = {}^3/_4$ concentration points (see also Appendix). In Table II we compare the interquartile widths with the computed interquartile widths, for the two forms $D_i(\phi)$ and for the three values of R. As with the qualitative comparison of the full profiles in Figures 2–4, the experimental interquartile widths in Table III correspond more closely to the theoretical values predicted on the basis of $D_2(\phi)$, especially at the lower R values.

At this point it is appropriate to consider a number of points relating to the validity of the comparison between our experiments and the various theoretical models. First, we note that the concentration of deuteriated polymer in our diffusion couples is at no point higher than 5%; this avoids possible problems associated with nonzero (positive) χ values, which can lead to a demixing effect,[25] or some reduction in the diffusion coefficient, as recently observed[26] for interdiffusion in polystyrene couples at a high (~50%) concentration of deuteriated species. Second, the length scales involved in the diffusion broadening are on the order of 500 μm; this is considerably larger than the length $l \simeq (D_B\tau_A)^{1/2}$, which even for the $3.2 \times 10^4/5.4 \times 10^5$ couple is only about 1 μm; that is, the diffusion time is well beyond the transient "swelling" regime.[14]

Finally, there is the possibility that "tube-renewal" effects may be playing a role in the diffusion process,[27] over and above reptation, especially for the $3.2 \times 10^4/5.4 \times 10^5$ couple (Figure 4), and that they could be responsible for the broadening in the N_B half of the couple (where the much longer N_A chains are essentially in a pure N_B medium). However, it is important to recall that even our shorter (N_B) chains are nonetheless much longer than the entanglement molecular weight ($N_B \simeq 27N_e$); in this case one may show, either from theory[27] or from experiment,[28] that the crossover value N_A^* beyond which tube-renewal effects are dominant is greater than the value of N_A in our experiments. Thus from ref 28b (where polystyrene melts were used) for a value $N_B = 27N_e$ the tube-renewal crossover can be extrapolated as $N_A^* \approx 600N_e$, while, for the 5.4×10^5 PBD-h sample, $N_A \simeq 450N_e$. Thus $N_A^* > N_A$ for all our couples, and tube-renewal is unlikely to dominate the dynamics.

We conclude that our experimental system provides a reasonable realization of the theoretical models for interdiffusion across an N_A/N_B couple where the A and B monomers are identical. Our results strongly indicate that the mutual diffusion coefficient is controlled by the mobility of the faster moving chains (as first proposed by Kramer and co-workers[13]) and thus suggest that for such a system the appropriate model may need to take account of convective effects, as proposed by Sillescu.[16]

Acknowledgment. Support by the SERC (E.A.J. and R.A.L.J.), ICI plc. (R.A.L.J.), and the Israeli Academy (J.K.) is gratefully acknowledged. This work was initiated following a stimulating talk at the Cavendish by Francoise Brochard some years ago. Comments and suggestions by K. Binder, F. Brochard, P.-G. de Gennes, E. J. Kramer, F. Miller, T. Nicholson, H. Sillescu, J. Sokolov, and M. Tirrell are gratefully acknowledged.

Appendix

For the one-dimensional geometry of our experiment we need to solve

$$\partial/\partial t[\phi(x,t)] = \partial/\partial x[D(\phi)\ \partial\phi/\partial x] \qquad \text{(A1)}$$

subject to the boundary conditions (for a unit step function at $t = 0$) $\phi(x) = 1$, $x = \infty$, and $\phi(x) = 0$, $x = -\infty$ at all t. We use the usual Boltzmann transformation of variables

$$z = x/(D_0t)^{1/2} \qquad \text{(A2)}$$

where D_0 is a constant with the dimensions of a diffusion coefficient, and set $\phi(x,t) = c(z)$, so that eq A1 becomes

$$-{}^1/_2z(dc/dz) = d/dz[(D(c)/D_0)\ dc/dz] \qquad \text{(A3)}$$

i.e., the interdiffusion coefficient is $D(c)$ in units of D_0. A simple iteration procedure to solve (A3) for $c(z)$ is as follows:[30] we guess a function $\Delta(z)$ such that

$$\Delta(z) = D(c(z))/D_0$$

Then from (A3),

$${}^1/_2(z\ dc/dz) + d/dz\ (\Delta(z)\ dc/dz) = 0 \qquad \text{(A4)}$$

An equivalent form of eq A4 may be written

$$d/dz\ (\Delta(z)e^{\Lambda(z)}\ dc/dz) = 0 \qquad \text{(A5)}$$

where

$$\Lambda = \int_0^z [z'/2\Delta(z')]\ dz'$$

and (A5) may be integrated once to give

$$dc/dz = (A/\Delta(z))e^{-\Lambda(z)}, \qquad A = \text{constant} \qquad \text{(A6)}$$

and integrated again to give

$$c(z) = B + \int_{-\infty}^z [A^{-\Lambda(z'')}\ dz''/\Delta(z')]$$

where B is another constant. Since our boundary conditions have $\phi(-\infty,t) = 0 = c(z=-\infty)$, we have $B = 0$, while A is fixed by the other boundary conditions, i.e., $c(+\infty) = 1$. Thus, making an initial guess for $\Delta(z)$, we find $c(z)$ and use it for an improved $\Delta(z)$.

For $D(\phi)$ varying as $D_1(\phi)$ or $D_2(\phi)$ we find that about 6–8 iterations of this procedure give a final self-consistent solution for the profile $c(z)$, when implemented on a BBC system B microcomputer. The midpoint of both theoretical and experimental curves was determined by ensuring that the "diffused" areas on either side of the midpoint (at $x = 0$) were equal (by numerical integration and by counting squares for theoretical and experimental profiles, respectively). The theoretical profiles were in addition "smeared" by convoluting the calculated curves

with the slit function corresponding to the slit width, estimated from initial step profiles as in Figure 1a; this smearing made little significant difference to the profile half-width. Profiles thus generated are essentially identical with those published by Brochard et al.[12] and by Kramer et al.[13] for the selected R values used by these authors. This procedure was used to generate the theoretical curves appearing in Figures 2–4.

The theoretical interquartile widths $W_{1/2}$ appearing in Table II were also computed by this numerical procedure. These provide an especially useful quantitative measure of the mutual diffusion coefficient controlling the broadening, for the following reason. For an initial step-function distribution whose subsequent diffusion broadening over a time t is controlled by a *concentration-independent* diffusion coefficient $D(\phi) = D_0$, the half-width $W_{1/2}$ of the resulting complementary error function, or erfc, profile is given by

$$W_{1/2} = \beta_0(4Dt)^{1/2}$$

where $\beta_0 = 1.10$ (to 3 sf). For the case of the *concentration-dependent* diffusion coefficients $D_1(\phi)$ and $D_2(\phi)$ the interquartile width may also be written as

$$W_{1/2} = \beta_{R,i}(4D_i(1/2)t)^{1/2}$$

where $\beta_{R,i}$ (i = 1 or 2) is a constant depending on R and on which of the two forms of $D_i(\phi)$ is applicable, and $D_i(1/2)$ is the value of D_i (for a given R) at $\phi = {}^1/_2$. The values of $\beta_{R,i}$ all turn out to be close to β_0 (even though the *shapes* of the curves are very different from an erfc profile), and, for a given R (within the range of the present study), are within a few percent of each other, as shown in Table III. Thus the experimental $W_{1/2}$ may be used to estimate the effective mutual diffusion coefficient $D(\phi={}^1/_2)$ characterizing the broadening at the interface. This observation (that the values of β are generally close to β_0) turns out to hold also for other forms of $D(\phi)$, as long as the concentration dependence of $D(\phi)$ is not too drastic.

References and Notes

(1) Klein, J. In *Encyclopedia of Polymer Science and Engineering*, 2nd ed.; Wiley: New York, 1987; Vol. 9, p 205. "*Macromolecular Dynamics*".
(2) de Gennes, P.-G. *Scaling Concepts in Polymer Physics*; Cornell University Press: Ithaca, NY, 1979.
(3) Doi, M.; Edwards, S. F. *The Theory of Polymer Dynamics*; Oxford University Press: Oxford, 1986.
(4) Gilmore, P. T.; Falabella R.; Lawrence R. L. *Macromolecules* **1980**, *13*, 880.
(5) Jones, R. A. L.; Klein, J.; Donald, A. M. *Nature (London)* **1986**, *321*, 161.
(6) Composto, R. J.; Mayer, J. W.; Kramer, E. J.; White, D. *Phys. Rev. Lett.* **1986**, *57*, 1312.
(7) Sokolov, J.; Jones, R.; Rafailovich, M.; Klein, J., unpublished results.
(8) (a) Murschall, U.; Fischer, E. W.; Herkt-Maetzky, Ch.; Fytas, G. *J. Polym. Sci., Polym. Lett. Ed.* **1986**, *24*, 191. (b) Brereton, M. G.; Fischer, E. W.; Fytas, G.; Murschall, U., submitted for publication to *J. Chem. Phys.*
(9) (a) Chalykh, A. Ye.; Saposhnikova, I. N.; Alliyev, A. D. *Vysokomol. Soedin., Ser. A* **1979**, *21*, 1664; *Polym. Sci. USSR (Engl. Transl.)* **1980**, *21*, 1835. (b) Kamenskii, A. N.; Fodiman, N. M.; Vogutskii, S. S. *Vysokomol. Soedin.* **1965**, *7*, 696.
(10) Flory, P. J. *Principles of Polymer Chemistry*; Cornell University Press: Ithaca, NY, 1953.
(11) (a) de Gennes, P.-G. *J. Chem. Phys.* **1980**, *72*, 4756. (b) Pincus, P. *Chem. Phys.* **1981**, *75*, 1996.
(12) Brochard, F.; Jouffroy, J.; Levinson, P. *J. Phys. Lett.* **1983**, *44*, L-455.
(13) Kramer, E. J.; Green, P. F.; Palmstrom, C. J. *Polymer*, **1984**, *25*, 473.
(14) Brochard, F.; de Gennes, P.-G. *Europhys. Lett.* **1986**, *1*, 221.
(15) Binder, K. *J. Colloid Polym. Sci.* in press.
(16) Sillescu, H. *Makrom. Chem. Rapid Commun.* **1984**, *5*, 519; (b) private communication.
(17) Ball, R., unpublished results.
(18) Jones, R. A. L. Ph.D. *Thesis*, Cambridge 1987.
(19) Rachapudy, H.; Smith, G. G.; Raju, V. R.; Graessley, W. W. *J. Polym. Sci: Poly. Phys.* **1979**, *17*, 1211.
(20) Klein, J.; Fletcher, D.; Fetters, L. *Faraday Symp. Chem. Soc.* **1983**, *18*, 159.
(21) Klein, J.; Briscoe, B. J. Proc. R. soc. London, **1979**, *365*, 53.
(22) Crank, J. *Mathematics of Diffusion*, 2nd ed.; Oxford University Press: Oxford 1975.
(23) Klein, J. *Philos. Mag. A* **1981**, *43*, 771.
(24) Bartels, C. R.; Crist, B.; Graessley, W. W. *Macromolecules* **1984**, *17*, 2702.
(25) Bates, F. S.; Wignall, G. D.; Koehler, W. C. *Phys. Rev. Lett.* **1985**, *55*, 2425. Bates, F. S.; Dierken, S. B.; Wignall, G. D. *Macromolecules* **1986**, *19*, 1938.
(26) Green, P. F.; Doyle, B. L. *Phys. Rev. Lett.* **1986**, *57*, 2407.
(27) Klein, J. *Macromolecules* **1986**, *19*, 105.
(28) (a) Green, P. F.; Mills, P. J.; Palmstrom, C. J.; Mayer, J. W.; Kramer, E. J. *Phys. Rev. Lett.* **1984**, *53*, 2145. (b) Green, P. F. Thesis, Department of Materials Science, Cornell University, 1986.
(29) Raju, V. R.; Menezes, E. V.; Marin, G.; Graessley, W. W.; Fetters, L. J. *Macromolecules* **1981**, *14*, 1668.
(30) Crank, J.; Henry, M. E. *Trans. Faraday Soc.* **1949**, *45*, 636, 1119. Also ref. 22, p 107.

Aperiodic Crystal Description of Diffusion in Concentrated Polymer–Solvent Systems

Randall W. Hall

Department of Chemistry, Louisiana State University, Baton Rouge, Louisiana 70803.

Received June 1, 1987

ABSTRACT: The aperiodic crystal picture is used to predict the solvent number fraction dependence of the mutual diffusion coefficient for two dense polymer–solvent systems. This theory, which has been applied successfully to diffusion in one component glasses, gives results that are distinct from previous free volume theories. The theory provides a way to calculate the free energy surface for a dense disordered system, from which the barrier heights to diffusion can be estimated.

Introduction

The diffusion of polymers in solvents and copolymers is an important and well-studied topic.[1] The formation of polymers is strongly dependent on the diffusion of molecules both into and out of the polymer, so the ability to predict diffusion rates would be of enormous importance to polymer chemists and engineers. The rate of polymerization is dependent on how fast monomer units, initiators, and other molecules can diffuse into the growing polymers, while further processing requires the low molecular weight residues to be removed. Thus, it is evident that efficient design of polymer synthesis requires an un-

0024-9297/88/2221-0239$01.50/0